Volume integral equation method for the analysis of scattered waves in an elastic half space

T. Touhei & K. Kuranami
Department of Civil Engineering, Tokyo University of Science, Japan

Abstract

A volume integral equation method for the analysis of scattered elastic waves in a half space is presented. This method introduces the generalized Fourier and its inverse transforms during the Krylov subspace iterative method for obtaining the solutions. The derivation of the coefficient matrix for the integral equation is not required. Furthermore, the introduction of the fast method for the generalized Fourier transform enables us to reduce the large amount of the CPU time, which was observed in the previous article. Numerical calculations are carried out to examine the effects of the fluctuations of the wave field due to the Lamé constants as well as the mass density on scattered waves. The numerical results are also compared with the results of the Born approximation to check the accuracy of the present method.
Keywords: analysis of scattered waves, elastic half space, volume integral equation, generalized Fourier transform, Krylov subspace iterative method.

1 Introduction

A type of the volume integral equation known as the Lippmann-Schwinger equation has been an efficient tool for theoretical investigation for the analysis of scattered waves in fields of the quantum mechanics [2] and acoustics [3]. The application of the volume integral equation to numerical analyses, however, is not very easy due to a requirement of a huge scale and dense matrix as a result of the discretization of the equation. Nevertheless, a number of applications of the volume integral equation to scattering problems are increasing. The application fields are extended to elastic wave as well as electro-magnetic wave propagations

WIT Transactions on Modelling and Simulation, Vol 50,
www.witpress.com, ISSN 1743-355X (on-line)
doi:10.2495/BE100221

(for example [4, 5]), in which methods to overcome the deficiency of the volume integral equation are formulated.

Previously, the first author of this article also showed a method for the volume integral equation for elastic wave propagation in a half space [1]. In the article, the generalized Fourier transform was developed for the wave field, which was applied to the Krylov subspace iterative method [6] to obtain the solution of the integral equation. The method was free from the derivation of a coefficient matrix for the integral equation, which consumed a vast amount of memory. A large amount of CPU time, however, was still observed for the analysis based on the proposed method [1]. Under the circumstances a method to resolve the requirement of a large CPU time has to be established.

In this article, a method to reduce the CPU time is presented. In addition, several numerical examples are also presented to investigate the reduction of the CPU time and properties of scattered waves due to the fluctuations of wave field by the Lamé constants as well as the mass density.

2 Method for scattering analysis

2.1 Volume integral equation

Consider a scattering problem shown in Fig. 1, in which a point source is applied to the free surface and scattered waves are caused due to the interaction between an incident wave and fluctuations of the wave field. A Cartesian coordinate system is employed to describe the wave field. For example, the spatial point is expressed as

$$x = (x_1, x_2, x_3) \in \mathbb{R}^3_+ \tag{1}$$

where x_3 is the vertical coordinate with the positive direction downward. The free surface boundary is denoted by $x_3 = 0$. The fluctuations of the wave field are expressed by Lamé constants and the mass density such that

$$\lambda(x) = \lambda_0 + \tilde{\lambda}(x) \tag{2}$$

$$\mu(x) = \mu_0 + \tilde{\mu}(x) \tag{3}$$

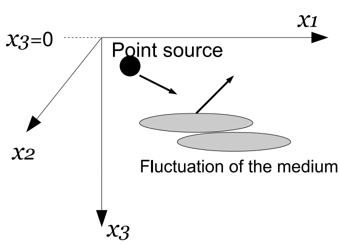

Figure 1: Concept of the analyzed model.

$$\rho(x) = \rho_0 + \tilde{\rho}(x), (x \in \mathbb{R}^3_+) \tag{4}$$

where λ_0, μ_0 and ρ_0 are the background Lamé constants and $\tilde{\lambda}$, $\tilde{\mu}$ and $\tilde{\rho}$ are their fluctuations.

The governing equations and the boundary conditions are expressed as

$$\Big(L_{ij} + \delta_{ij}\rho_0\omega^2\Big)u_j(x) = N_{ij}u_j(x) - q_i\delta(x - x_c) \tag{5}$$

$$P_{ij}u_j(x) = 0, \quad \text{at } x_3 = 0 \tag{6}$$

where, L_{ij} is the Navier differential operator, N_{ij} is the differential operator constructed by the fluctuations of the wave field, δ_{ij} is Kronecker's delta, $\delta(\cdot)$ is the Dirac delta function, q_i is amplitude of the point source and x_c is the point where the point source is applied. The explicit forms of L_{ij}, N_{ij} are given by

$$L_{ij} = (\lambda_0 + \mu_0)\partial_i\partial_j + \delta_{ij}\mu_0\partial_k^2 \tag{7}$$

$$\begin{aligned} N_{ij} = &-(\tilde{\lambda}(x) + \tilde{\mu}(x))\partial_i\partial_j - \delta_{ij}\tilde{\mu}(x)\partial_k^2 \\ &- (\partial_i\tilde{\lambda}(x))\partial_j - \delta_{ij}(\partial_k\tilde{\mu}(x))\partial_k - (\partial_j\tilde{\mu}(x))\partial_i - \delta_{ij}\tilde{\rho}(x)\omega^2 \end{aligned} \tag{8}$$

$$[P_{ij}] = \begin{pmatrix} \mu(x)\partial_3 & 0 & \mu(x)\partial_1 \\ 0 & \mu(x)\partial_3 & \mu(x)\partial_2 \\ \lambda(x)\partial_1 & \lambda(x)\partial_2 & \big(\lambda(x) + 2\mu(x)\big)\partial_3 \end{pmatrix} \tag{9}$$

The solution of Eq. (5) together with the boundary condition shown in Eq. (9) can be expressed by the following volume integral equation:

$$u_i(x) = G_{ij}(x, x_c)q_j - \int_{\mathbb{R}^3_+} G_{ij}(x, y)N_{jk}u_k(y)dy \tag{10}$$

where $G_{ij}(x, y)$ is Green's function for an elastic half space defined by

$$\Big(L_{ij} + \delta_{ij}\rho_0\omega^2\Big)G_{jk}(x, y) = -\delta_{ik}\delta(x - y) \tag{11}$$

together with the following boundary condition:

$$P^{(0)}_{ij}G_{jk}(x, y) = 0 \text{ (at } x_3 = 0) \tag{12}$$

where operator $P^{(0)}_{ij}$ is given as:

$$[P^{(0)}_{ij}] = \begin{pmatrix} \mu_0\partial_3 & 0 & \mu_0\partial_1 \\ 0 & \mu_0\partial_3 & \mu_0\partial_2 \\ \lambda_0\partial_1 & \lambda_0\partial_2 & \big(\lambda_0 + 2\mu_0\big)\partial_3 \end{pmatrix} \tag{13}$$

The volume integral equation in terms of the scattered wave field $v_i(x)$

$$v_i(x) = u_i(x) - G_{ij}(x, x_c)q_j \tag{14}$$

is expressed by

$$v_i(x) = -\int_{\mathbb{R}^3_+} G_{ij}(x, y)N_{jk}v_k(y)dy - \int_{\mathbb{R}^3_+} G_{ij}(x, y)N_{jk}G_{kl}(x, x_c)q_l dy \tag{15}$$

2.2 A method for the volume integral equation based on the generalized Fourier transform

The generalized Fourier and its inverse transforms [1] are used for solving the volume integral equation shown in Eq. (15). These transforms are given respectively in the following forms:

$$\mathscr{U}_{ij}f_j(x) = \int_{\mathbb{R}^3_+} \Lambda^*_{ji}(\xi, x)f_j(x)dx \tag{16}$$

$$\mathscr{U}^{-1}_{ij}\hat{f}_j(\xi) = \int_{\mathbb{R}^2} \sum_{\xi\in\sigma_p} \Lambda_{ij}(\xi, x)\hat{f}_j(\xi)d\xi_1 d\xi_2 + \int_{\mathbb{R}^2}\int_{\xi_r}^{\infty} \Lambda_{ij}(\xi, x)\hat{f}_j(\xi)d\xi_3 d\xi_1 d\xi_2 \tag{17}$$

where $\Lambda_{ij}(\xi, x)$ is kernel of generalized Fourier transform satisfying the following equation:

$$L_{ij}\Lambda_{jk}(\xi, x) = -\mu_0\xi_3^2\Lambda_{ik}(\xi, x)$$
$$P^{(0)}_{ij}\Lambda_{jk}(\xi, x) = 0, \quad \text{at } x_3 = 0 \tag{18}$$

and the subscript $*$ for $\Lambda_{ij}(\xi, x)$ denotes the complex conjugate. Note that ξ for $\Lambda_{ij}(\xi, x)$ is the wavenumber vector having components

$$\xi = (\xi_1, \xi_2, \xi_3) \in \sigma_p \cup \sigma_c \tag{19}$$

and ξ_r in Eq. (17) is denoted by

$$\xi_r = \sqrt{\xi_1^2 + \xi_2^2} \tag{20}$$

where σ_p and σ_c denote the set of the wavenumber for the Rayleigh wave and body waves, respectively, defined by

$$\sigma_p = \{\ \xi \in \mathbb{R}^3_+ \mid (2\xi_r^2 - \xi_3^2)^2 - 4\xi_r^2\gamma\nu = 0\}$$

www.witpress.com, ISSN 1743-355X (on-line)

$$\sigma_c = \{\ \xi \in \mathbb{R}^3_+ \mid \xi_3 > \xi_r\} \tag{21}$$

In Eq. (21), γ and ν are defined by

$$\gamma = \sqrt{\xi_r^2 - \xi_3^2(c_T/c_L)^2}$$
$$\nu = \sqrt{\xi_r^2 - \xi_3^2} \tag{22}$$

where c_T and c_L are the S and P wave velocities in the background structure. The explicit forms of $\Lambda_{ij}(\xi, x)$ are very complicated and given in the article [1]. Therefore, due to the limitation of the length of the manuscript, the details of the description of $\Lambda_{ij}(\xi, x)$ are omitted here.

There is an orthogonality relation for the kernel of the generalized Fourier transform $\Lambda_{ij}(\xi, x)$ expressed by

$$\int_{\mathbb{R}^3_+} \Lambda^*_{ji}(\xi', x)\Lambda_{jk}(\xi, x)dx = \delta_{ik}\delta(\xi_1 - \xi'_1)\delta(\xi_2 - \xi'_2) \tag{23}$$

when $\xi, \xi' \in \sigma_p$ and

$$\int_{\mathbb{R}^3_+} \Lambda^*_{ji}(\xi', x)\Lambda_{jk}(\xi, x)dx = \delta_{ik}\delta(\xi_1 - \xi'_1)\delta(\xi_2 - \xi'_2)\delta(\xi_3 - \xi'_3) \tag{24}$$

when $\xi, \xi' \in \sigma_c$.

Applications of the generalized Fourier transform to the volume integral equation leads to the following:

$$\hat{v}_i(\xi) = -\hat{h}(\xi)\mathscr{U}_{ij}N_{jk}\mathscr{U}^{-1}_{kl}\hat{v}_l(\xi) - \hat{h}(\xi)\mathscr{U}_{ij}N_{jk}G_{kl}(x, x_c)q_l \tag{25}$$

where $\hat{v}_i(\xi)$ is the generalized Fourier transform of $v_i(x)$ and $\hat{h}(\xi)$ is the function related to the generalized Fourier transform of the Green's function expressed by

$$\hat{h}(\xi) = \frac{1}{\mu_0\xi_3^2 - \rho_0\omega^2 + i\varepsilon} \tag{26}$$

Note that ε in Eq. (26) is an infinitesimally small positive number. Equation (25) can be regarded as the Fredholm equation of the second kind. In an actual situation of the numerical calculations, the generalized Fourier and its inverse transforms are discretized, so that the Eq. (25) becomes the equation in the finite dimensional vector space to which the Krylov subspace iterative method can be applied. In the previous article [1], the trapezoidal formula is applied to the discretization of the transform with respect to the vertical coordinate system. As a result, a large amount of CPU time was required for numerical calculations, even if FFT2D was incorporated into the horizontal coordinate system.

In this article, to reduce the CPU time, the kernel of the generalized Fourier transform with respect to the vertical coordinate system is decomposed into the

Fourier cosine, sine and Laplace transforms, to that fast algorithms can be applied. For the fast Laplace transform, a method by Strain [7] is introduced here. By means of the above method for the vertical coordinate system and FFT2D for the horizontal coordinate system, a fast algorithm for the generalized Fourier transforms can be established. The following numerical examples are based on the fast method. Note that the present approach is free from the derivation of the coefficient matrix which becomes huge scale and dense.

3 Numerical examples

In this article, numerical calculations are carried out for three cases. The first case (case-1) takes into account the fluctuations of the Lamé constants and the next case (case-2) takes into account the fluctuations of the mass density. The last case (case-3) considers both the fluctuations of the Lamé constants as well as the mass density. Those fluctuations for the Lamé constants and the mass density are shown in Fig. 2. As can be seen in Fig. 2, the maximum amplitudes of the fluctuations of the Lamé constants are 0.1 GPa, while that of the mass density is 0.1 $\mathrm{g/cm}^3$. The fluctuated areas spreads to areas whose radius is around 3 km.

The background structure of an elastic half space is set by $\lambda_0 = 4.0[\mathrm{GPa}]$, $\mu_0 = 2.0[\mathrm{GPa}]$ and $\rho_0 = 2.0[\mathrm{g/cm}^3]$. For the discretization of the generalized Fourier transform, the intervals of the grids in the space domain are set by $\Delta x_j = 0.25$ km, $(j = 1, 2, 3)$. The relationship of the grids in the space domain and the wavenumber space are given as

$$\Delta x_j \Delta \xi_j = \frac{2\pi}{N_j} \quad (j = 1, 2)$$
$$\Delta x_3 \Delta \bar{\nu} = \frac{2\pi}{N_3} \tag{27}$$

where $N_j, (j = 1, 2, 3)$ is the number of grids for the j-th coordinate, $\Delta\xi_1$ and $\Delta\xi_2$ are the intervals of the horizontal grids in the wavenumber domain and $\Delta\bar{\nu}$

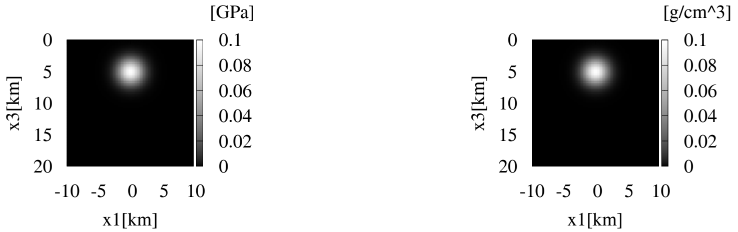

(a) the Lamé constants (b) the mass density

Figure 2: Fluctuation of the wave field.

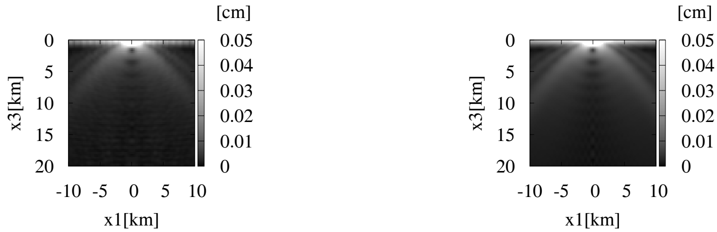

(a) generalized Fourier transform (b) Hankel transform

Figure 3: Comparison of the incident wave field.

defines the parameter for the interval of the grids for ξ_3 such that

$$\xi_3 = \sqrt{\xi_r^2 + n^2 \Delta \bar{\nu}^2}, \ \ (0 \leq n \leq N_3 - 1) \tag{28}$$

A method for discretizing ξ_3 is not very simple, which is due to decomposing the integration with respect to ξ_3 into the discrete Fourier and Laplace transform [8]. In this numerical example, $N_j, (j = 1, 2, 3)$ is set by 256.

Figures 3(a) and (b) show the comparison of the incident wave field for scattering analyses, in which the amplitudes of the displacement field is described. The incident wave field is constructed by the fast generalized Fourier transform for Fig. 3(a), while that is constructed by the Hankel transform for Fig. 3(b). The point source for the incident wave field is applied to a surface of the elastic half space. The amplitude of the point source is 1.0×10^{10}N, the direction is vertical and the excitation frequency is 1.0 Hz. It is found from Figs. 3(a) and (b) that the both results show good agreements, which verifies the accuracy of the fast generalized Fourier transform. The regions for the high displacement amplitudes can be seen in Fig. 3.

These regions are along the free surface boundary and towards the downward direction showing a strong directionality, which are for the Rayleigh wave and the body waves, respectively.

Figures 4(a)-(c) show the displacement amplitude of the scattered waves in $x_1 - x_3$ plane for cases 1 to 3. The Bi-CGSTAB method as the Krylov subspace iterative method is used to obtain the solutions of the volume integral equation. It is found from Fig. 4(a) that high displacement amplitude areas are found to spread mainly in the region where the propagation of the body waves can be seen. The highest displacement amplitudes are recognized just outside the fluctuated zone where the wave velocities are higher than those of the surroundings. The reason for this is that the reflections of the waves form the fluctuated zone are caused. According to Fig. 4(b), the displacement amplitudes are higher than those shown in Fig. 4(a). The reason is that the wave velocities of the fluctuated zone are lower than those of the surrounding due to the fluctuation of the mass density. As a result, waves are amplified inside the fluctuated zone. It is found from Fig. 4(c) that the

www.witpress.com, ISSN 1743-355X (on-line)

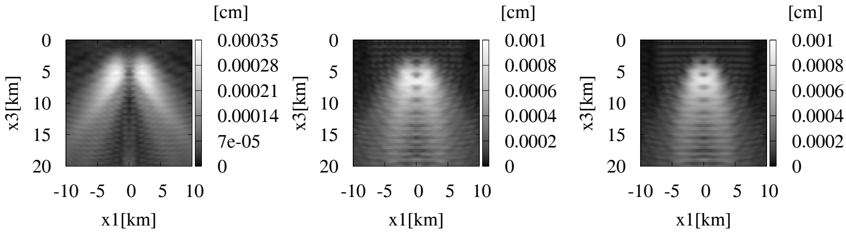

(a) case 1 (b) case 2 (c) case 3

Figure 4: Displacement amplitudes of scattered waves in a vertical plane by the present method.

high displacement amplitude areas are slightly narrower than the results of case 2. The reason is that the contrast of the wave velocities inside the fluctuated zones to those of the surroundings become smaller than those of case 2.

For the comparison of the above results, the scattered waves obtained from the Born approximation are shown in Figs. 5(a)-(c). The equation for the Born approximation is as follows:

$$v_i(x) = -\int_{\mathbb{R}^3_+} G_{ij}(x,y) N_{jk} G_{kl}(x,x_c) q_l dy \tag{29}$$

which is according to Eq. (15). It is found from Fig. 5 that the displacement amplitudes due to the Born approximations are almost the same as the results due to the present method. The agreement of the results provided by the present method and the Born approximation show that the fluctuations used in the present study are not very large. In addition, the above agreement also strengthen the accuracy of the present method.

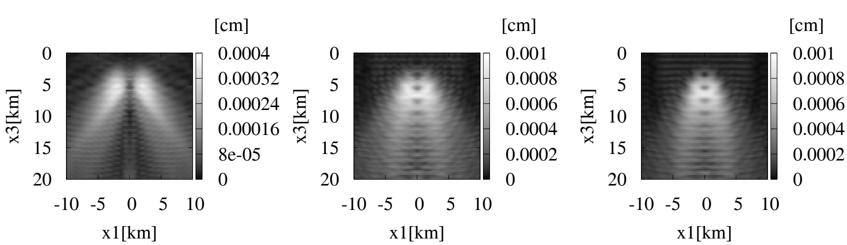

(a) case 1 (b) case 2 (c) case 3

Figure 5: Displacement amplitudes of scattered waves in a vertical plane by the Born approximation.

www.witpress.com, ISSN 1743-355X (on-line)

The numerical calculations were carried out here by a computer with an AMD Opteron 2.4 GHz processor. The CPU time needed for the present example based on the Bi-CGSTAB method was around 35 min. The introduction of the fast algorithm are found to enable us to reduce the large amount of CPU time recognized in the previous article [1], that was 15 hours.

4 Conclusion

In this article, scattered waves were analyzed by means of the volume integral equation method. The starting point of the formulation was the volume integral equation in the wavenumber domain, to which the generalized Fourier and its inverse transforms were repeatedly applied during the Krylov subspace iterative method. The method did not require the derivation of the coefficient matrix for the integral equation. In addition, the introduction of the fast method was found to enable us to reduce the large amount of the CPU time, which was observed in the previous article [1]. The numerical calculations were carried out to examine the effects of the fluctuations of the wave field by Lamé constants as well as the mass density on scattered waves. According to the numerical results, the properties of the scattered waves were well explained by the wave velocities inside as well as surroundings of the fluctuated area. In addition, the effectiveness of the Born approximation to the present numerical model was also verified.

References

[1] Touhei, T. (2009). Generalized Fourier transform and its application to the volume integral equation for elastic wave propagation in a half space, *International Journal of Solids and Structures*, **46**, 52-73.

[2] Ikebe, T. (1960). Eigenfunction expansion associated with the Schroedinger operators and their applications to scattering theory, *Arch. Rat. Mech. Anal.*, **5**, 1-34.

[3] Colton, D. and Kress, R. (1998). *Inverse acoustic and electromagnetic scattering theory*, Berlin, Springer.

[4] De Zaeytijd,J., Bogaert,I. and Franchois, A. (2008). An efficient hybrid MLFMA-FFT solver for the volume integral equation in case of sparse 3D inhomogeneous dielectric scatterers, *Journal of Computational Physics*, **227**, 7052-7068.

[5] Yang, J., Abubaker, A., van den Berg, P.M., Habashy, T.M. and Reitich, F. (2008). A CG-FFT approach to the solution of a stress-velocity formulation of three-dimensional scattering problems, *Journal of Computational physics*, **227**, 10018-10039.

[6] Barrett, M., Berry, M., Chan, T.F., Demmel, J., Donato, J. M., Dongarra, J., Eijkhout, V., Pozo, R., Romine, C. and Van der Vorst, H. (1994). *Templates for the solution of Linear Systems: Building Blocks for Iterative Methods*, break SIAM.

www.witpress.com, ISSN 1743-355X (on-line)

[7] Strain, J. (2000). A fast Laplace transform based on Laguerre functions *Courant Institute of Mathematical Sciences*.
[8] Touhei, T., Takagishi, T. and Wajima, Y. (2009), Analysis of scattered elastic waves in a half space by means of the volume integral equation method. *Journal of Applied Mechanics, (JSCE)*, **12**, 27-34, in Japanese.